Different top-down approaches to two-dimensional nanoparticles with plate-like geometry

Cornelia Damm[1*], Paola Cardenas Lopez[1,2], Johannes Walter[1,2], Bettina Winzer[1], Moritz Moß[1,2], Wolfgang Peukert[1,2]

[1]Institute of Interfaces and Particle Technology (IPT), Friedrich-Alexander-Universität Erlangen-Nürnberg (FAU), Cauerstr. 4, D-91058 Erlangen, Germany
[2]Center for Functional Particle Systems, Friedrich-Alexander-Universität Erlangen-Nürnberg (FAU), Haberstr. 9a, D-91058 Erlangen, Germany

Abstract. We present two approaches for production of two-dimensional (2D) nanoparticles with plate-like geometry in a stirred media mill. The first method is stirred media delamination. It relies on overcome of weak van-der-Waals interactions between the layers of layered materials due to shear forces generated by collisions of the particles with the milling beads. This results in delamination of nanosheets with a thickness of few atomic layers from layered materials. The second method for nanoplatelet generation is based on plastic deformation of ductile particles in a stirred media mill by compression forces. Process parameter studies for production of 2D nanomaterials require fast in-suspension particle size analytics with high statistical significance. Generally, in-suspension size analysis of 2D nanoparticles is challenging. Size-distributions of 2D nanomaterials with size- and shape-dependent optical properties can be measured by Analytical Ultracentrifugation with multiwavelength detector (MWL-AUC). For nanomaterials without size-dependent light absorption, scattering of a laser beam in forward and sideward direction can be exploited to distinguish between nanoparticles of different geometry.

1. MoS_2 nanosheet formation by stirred media delamination

2D nanomaterials with plate-like geometry like graphene, MoS_2, WS_2 or GeS exhibit unique optical and electronic properties and are therefore, promising for applications as visible light photocatalysts, for Li-ion batteries and sensing [1-3].

Delamination of sheets with a thickness of only few atomic layers from layered materials in liquid phase is a versatile approach to plate-like 2D nanoparticles. In layered materials there are strong covalent and/or ionic bonds within the layers, but only weak van-der-Waals interactions between the layers. The van-der-Waals forces between the layers can be overcome by applying shear forces parallel to the layers. In this way thin nanosheets are peeled-off. If the delaminated nanosheets are sufficiently stabilized against agglomeration and re-stacking, suspensions of nanosheets are accessible by liquid phase delamination processes. The shear forces required for delamination of layered materials can be generated by ultrasound [4], by rotor-stator devices [5], high pressure homogenization [6] and stirred media mills [7-11]. We investigated the stirred media delamination of layered materials in detail for graphene [6-9], hexagonal boron nitride [10] and molybdenum disulfide [11] as this method is in principle scalable to industrial relevant amounts of material. We found that for sufficiently low stressing energy of the milling beads delamination of nanosheets dominates over lateral fracture [8].

In this contribution, we show the delamination of molybdenum disulfide in a stirred media mill as this material is an interesting semiconductor with size-dependent optical properties [12], see Figure 1.

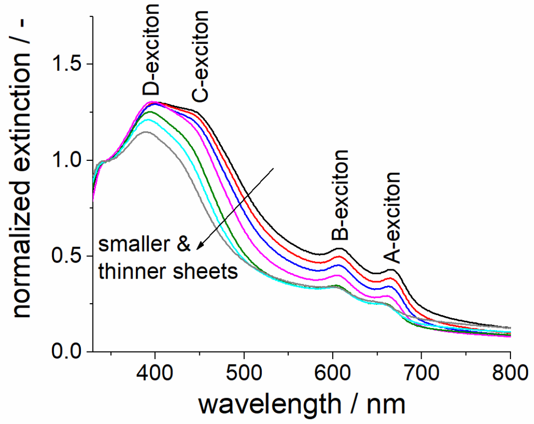

Figure 1. Size-dependent UV/Vis spectra of molybdenum disulfide nanosheets with excitonic transitions [11].

Backes et al. exploited the size-dependent optical properties of molybdenum disulfide nanosheets to develop a method for determination of mean values for

* Corresponding author: cornelia.damm@fau.de

the lateral diameter L and for the number of layers per particle N [13]. By correlating UV/Vis spectra of different molybdenum disulfide size fractions with the nanosheet dimensions obtained from statistical TEM and AFM analyses they obtained the following empirical equations [13]:

$$L = \frac{3.5\ \mu m \cdot \frac{E_B}{E_{345}} - 0.14\ \mu m}{11.5 - \frac{E_B}{E_{345}}} \quad (1)$$

$$N = 2.3 \cdot 10^{36} \cdot e^{-\frac{54888\ nm}{\lambda_A}} \quad (2)$$

with E_{345nm}: extinction at 345 nm, E_B: extinction at the B-exciton and λ_A: wavelength of the A-exciton (see Figure 1).

We demonstrate, how to extend the method of Backes et al. so that distributions for L and N can be obtained. For that purpose, we classified the delaminated samples from the stirred media mill by centrifugation to different sphere-equivalent cut-sizes to obtain different size-fractions. These size fractions were analysed by MWL-AUC, which is the gold standard for size and shape analytics in suspension [14-16]. As this method yields the distribution of the sedimentation coefficient (sedimentation rate normalized to the relative centrifugal force) in combination with the UV/Vis spectrum of each settling component of the sample, distributions for L and N can be extracted from a single AUC measurement.

Based on the distributions for L and N obtained from MWL-AUC, the classification by preparative centrifugation is described quantitatively by determination of a separation efficiency curve for each size dimension.

2. Plastic deformation of spherical silica particles

Compression experiments on single particles in a SEM micomanipulator revealed that spherical silica particles with sizes below a critical value – the brittle-ductile-transition – do not show brittle fracture when exposed to compression forces. Instead, the shape of the particles transforms from spherical to plate-like due to plastic deformation. During processing in a stirred media mill, particles are exposed to compression forces when captured between two colliding milling beads. As expected from SEM micromanipulation, the formation of plate-like silica nanoparticles in a stirred media mill is observed for feed particles with sizes in the ductile range [17]. We processed spherical amorphous silica particles in an organic dispersing medium in a stirred media mill to prevent dissolution. The size of the feed particles and the process conditions were varied. The shape transformation from spherical to plate-like was investigated by statistical analysis of SEM micrographs as well as in suspension by single-particle light scattering in forward (FSC) and sideward (SSC) direction, see Figure 2.

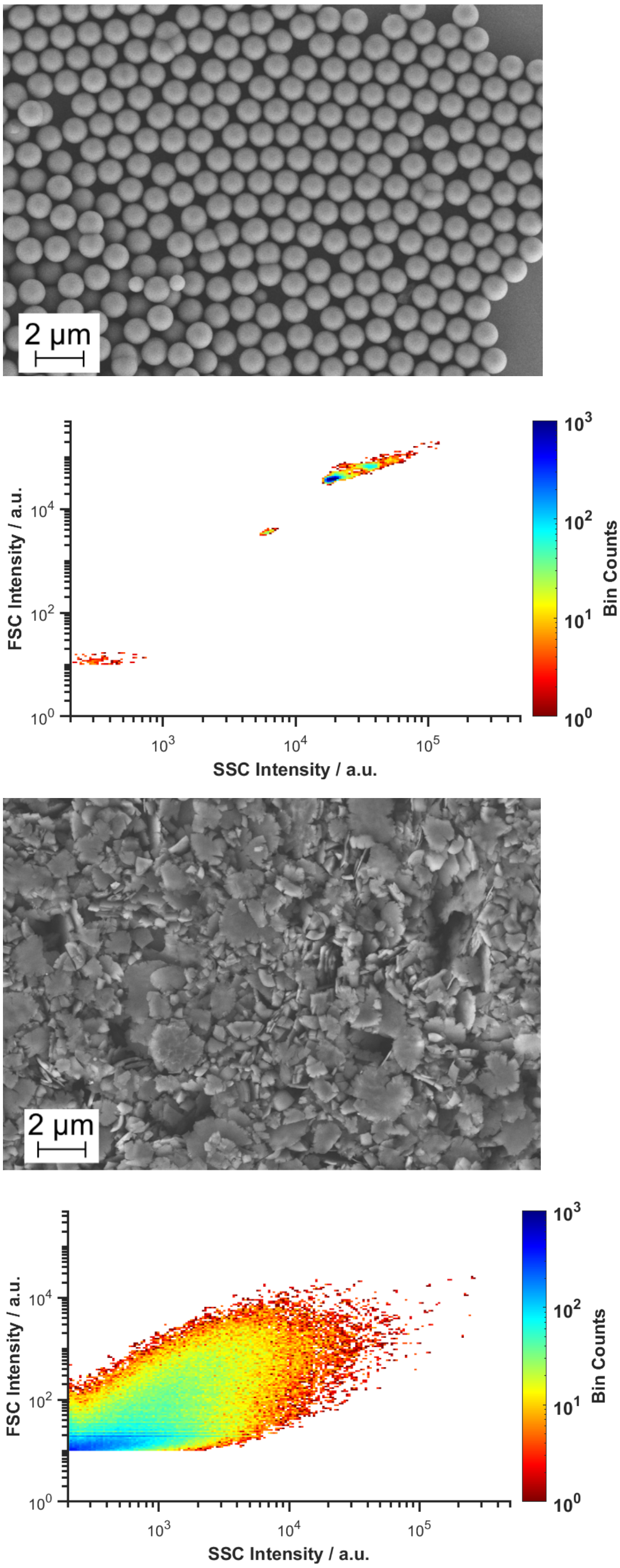

Figure 2. SEM micrograph and 2D scatter histogram of the spherical feed particles (above) and of plate-like particles formed by plastic deformation in a stirred media mill (below).

Within 10 h the spherical particles are completely transformed to platelets with a thickness of about 100 nm or even thinner. As the light scatter behaviour of spherical and plate-like silica particles is quite different, see Figure 2, a quantitative evaluation of the scatter histograms provides access to the relative fraction of spheres and platelets in the sample. The used laser light scattering device "LUMiSPOC" (Single-Particle Optical Counter from LUM GmbH) enables analysis of the scatter behaviour of thousands of particles within few minutes. Thus, this method provides fast shape analysis in suspension with high statistical significance and will be further developed for more detailed size and shape analysis in future.

Acknowledgement
The authors gratefully acknowledge the financial support of this work by the German Science Foundation (DFG) within the priority program PP2045 – Highly specific and multi-dimensional fractionation of particle systems with technical relevance and the collaborative research center CRC1411 – Design of particulate products as well as in project PE427/40-1.

References

[1] Novoselov, K.S., Geim, A.K., Morozov, S.V., Jiang, D., Zhang, Y., Dubonos, S.V., Grigorieva, I.V., & Firsov, A. A. et al., (2004) Electric Field Effect in Atomically Thin Carbon Films. *Science* 5696, 666–669.

[2] Wang, Z. & Mi, B., (2017) Environmental applications of 2D molybdenum disulfide (MoS_2) nanosheets. *Environmental Science & Technology* 51, 8229-8244.

[3] Boland, J.B., Tian, R., Harvey, A., Vega-Mayoral, V., Griffin, A., Horvath, D.V., Cabbett, C., Breshears, M., Pepper, J., Li, Y., & Coleman, J. N., (2020) Liquid phase exfoliation of GeS nanosheets in ambient conditions for lithium ion battery applications. *2D Mater.* 7, 35015.

[4] Guardia, L., Fernandez-Merino, M.J., Paredes, J.I., Solis-Fernandez, P., Villar-Rodil, S., & Martinez-Alonso, A. et al., (2011) High-throughput production of pristine graphene in an aqueous dispersion assisted by non-ionic surfactants. *Carbon* 49, 1653–1662.

[5] Paton, K.R., Varrla, E., Backes, C., Smith, R.J., Khan, & U., O'Neill, A. et al., (2014) Scalable production of large quantities of defect-free few-layer-graphene by shear exfoliation in liquids. *Nat. Mater.* 13, 624–630.

[6] Nacken, T.J., Damm, C., Walter, J., Rüger, A., Peukert, W., (2015) Delamination of graphite in a high pressure homogenizer. *RSC Adv.* 5, 57328–57338.

[7] Knieke, C., Berger, A., Voigt, M., Taylor, R., Röhrl, J., & Peukert, W., (2010) Scalable production of graphene sheets by mechanical delamination. *Carbon* 48, 3 196–3204.

[8] Nacken, T. J., Damm, C., Xing, H., Rüger, A., & Peukert, W., (2015) Determination of quantitative structure-property and structure-process relationships for graphene production in water. *Nano Research* 8, 1865–1881.

[9] Damm, C., Nacken, T. J., & Peukert, W., (2015) Quantitative evaluation of delamination of graphite by wet media milling. *Carbon* 81, 284–294.

[10] Damm, C., Körner, J., & Peukert, W., (2013) Delamination of hexagonal boron nitride in a stirred media mill. *J. Nanopart. Res.* 15, 1561, 1561.

[11] Damm, C., Long, D., Walter, J., & Peukert, W., (2024) Size and Shape Selective Classification of Nanoparticles. *Powders* 3, 255–279.

[12] Mak, K.F., Lee, C., Hone, J., Shan, J. & Heinz, T. F., (2010) Atomically thin MoS_2: a new direct-gap semiconductor. *Physical Review Letters* 105, 136805.

[13] Backes, C., Smith, R. J., McEvoy, N., Berner, N. C., McCloskey, D., Nerl, H. C., O'Neill, A., King, P. J., Higgins, T., Hanlon, D., Scheuschner, N., Maultzsch, J., Houben, L., Duesberg, G. S., Donegan, J. F., Nicolosi, V., & Coleman, J. N., (2014) Edge and confinement effects allow in situ measurement of size and thickness of liquid-exfoliated nanosheets. *Nature Communications* 5, 4576.

[14] Walter, J., Löhr, K., Karabudak, E., Reis, W., Mikhael, J., Peukert, W., Wohlleben, W., & Cölfen, H. (2014) Multidimensional analysis of nanoparticles with highly disperse properties using multiwavelength analytical ultracentrifugation. *ACS Nano* 8, 8871–8886.

[15] Walter, J., Sherwood, P.J., Lin, W., Segets, D., Stafford, W. F., & Peukert, W. (2015) Simultaneous analysis of hydrodynamic and optical properties using analytical ultracentrifugation equipped with multiwavelength detection. *Analytical Chemistry* 87, 3396–3403.

[16] Wawra, S. E., Pflug, L., Thajudeen, T., Kryschi, C., Stingl, M., & Peukert, W. (2018) Determination of the two-dimensional distributions of gold nanorods by multiwavelength analytical ultracentrifugation. *Nature Communications* 9, 4898.

[17] Esper, J. D., Liu, L., Willnauer, J., Strobel, A., Schwenger, J., & Peukert, W., (2020) Scalable production of glass flakes via compression in the liquid phase. *Advanced Powder Technology* 31, 4145-4156.